Supporting Information

Zn_3P_2-Zn_3As_2 Solid Solution Nanowires

Hyung Soon Im,[†] Kidong Park,[†] Dong Myung Jang,[†]Chan Su Jung,[†] Jeunghee Park,[†*] Seung Jo Yoo,[‡] and Jin-Gyu Kim[‡]

[†]*Department of Chemistry, Korea University, Jochiwon 339-700, Korea;* [‡]*Division of Electron Microscopic Research, Korea Research Institute of Standards and Science, Daejeon 305-806, Korea*

Table S1. Summary of characteristics of previous Zn_3P_2 and Zn_3As_2 NW photodetectors.

Reference	NW	Wavelength (nm)	Light Intensity	Photocurrent (ΔI)	S[a]	On/off ratio[b]	R (A/W)[c]	G (%)[d]
29	Zn_3P_2	680	< 5 mW	0.9 nA at 1V		3		
		532	< 5 mW	0.5 nA at 1V		4		
		white		0.3 nA at 1V		2.5		
32	Zn_3P_2	325	2.7~97.8 mW/cm^2	3 nA at 1 V (at 4.3 mW/cm^2)				
		488		4 nA at 1 V (at 4.3 mW/cm^2)				
		633		7 nA at 1 V (at 4.3 mW/cm^2) Max. 150 nA (at 97.8 mW/cm^2)	100			470
33	Zn_3P_2	620	0.4-0.9 mW/cm^2	1.1 μA at 2 V (at 0.7 mW/cm^2)			600	1200
		580		1 μA				
		520		0.9 μA				
		480		0.8 μA				
		420		0.6 μA				
		350		0.4 μA				
35	Zn_3As_2	460-470	0.73-2.52 mW/cm^2	0.05 μA at 2 V		2.75		
		520-530		0.1 μA		2.25		
		White		0.15 μA				

[a] S = Photosensitivity = $(I_{light} - I_{0(=dark)})/I_0 = \Delta I/I_0$, where ΔI is photocurrent.
[b] On-off ratio = I_{light}/ I_0
[c] R (A/W) = Responsitivity = ΔI/PS, where ΔI = photocurrent, P = light intensity, S = area
[d] G = Gain = number of electrons detected per incident photon = (ΔI/P) (hν/q); hν = photon energy, q = electron charge

Table S2. Summary of experimental conditions for the synthesis of $Zn_3(P_{1-x}As_x)_2$ NWs.

No.	$Zn_3(P_{1-x}As_x)_2$	x	Source[a]					Temperature (°C)		Catalysts
			Zn_3P_2	Zn_3As_2	Zn	InP	InAs	Source	Substrate	
1	S-$Zn_3(P_{1-x}As_x)_2$	0	1	0	0	0	0	700-800	500-550	Au
2		0.2	0.8	0.2	0	0	0			
3		0.3	0.7	0.3	0	0	0			
4		0.5	0.45	0.55	0	0	0			
5		0.7	0.25	0.75	0	0	0			
6		0.8	0.15	0.85	0	0	0			
7		1	0	1	0	0	0			
8	T-$Zn_3(P_{1-x}As_x)_2$	0	0	0	1	0	1	800-900	600-650	In
9		0.1	0	0	1	0.2	0.8			
10		0.5	0	0	1	0.5	0.5			
11		0.9	0	0	1	0.8	0.2			
12		1	0	0	1	0	1			

[a] Weight ratio of source with a total weight of 30~40 mg.

Figure S1. SEM images of the cross-sectional view of the S-$Zn_3(P_{1-x}As_x)_2$ NWs; EDX spectra of S-$Zn_3(P_{1-x}As_x)_2$ NWs: x = 0, 0.2, 0.3, 0.6, 0.7, 0.8, and 1.

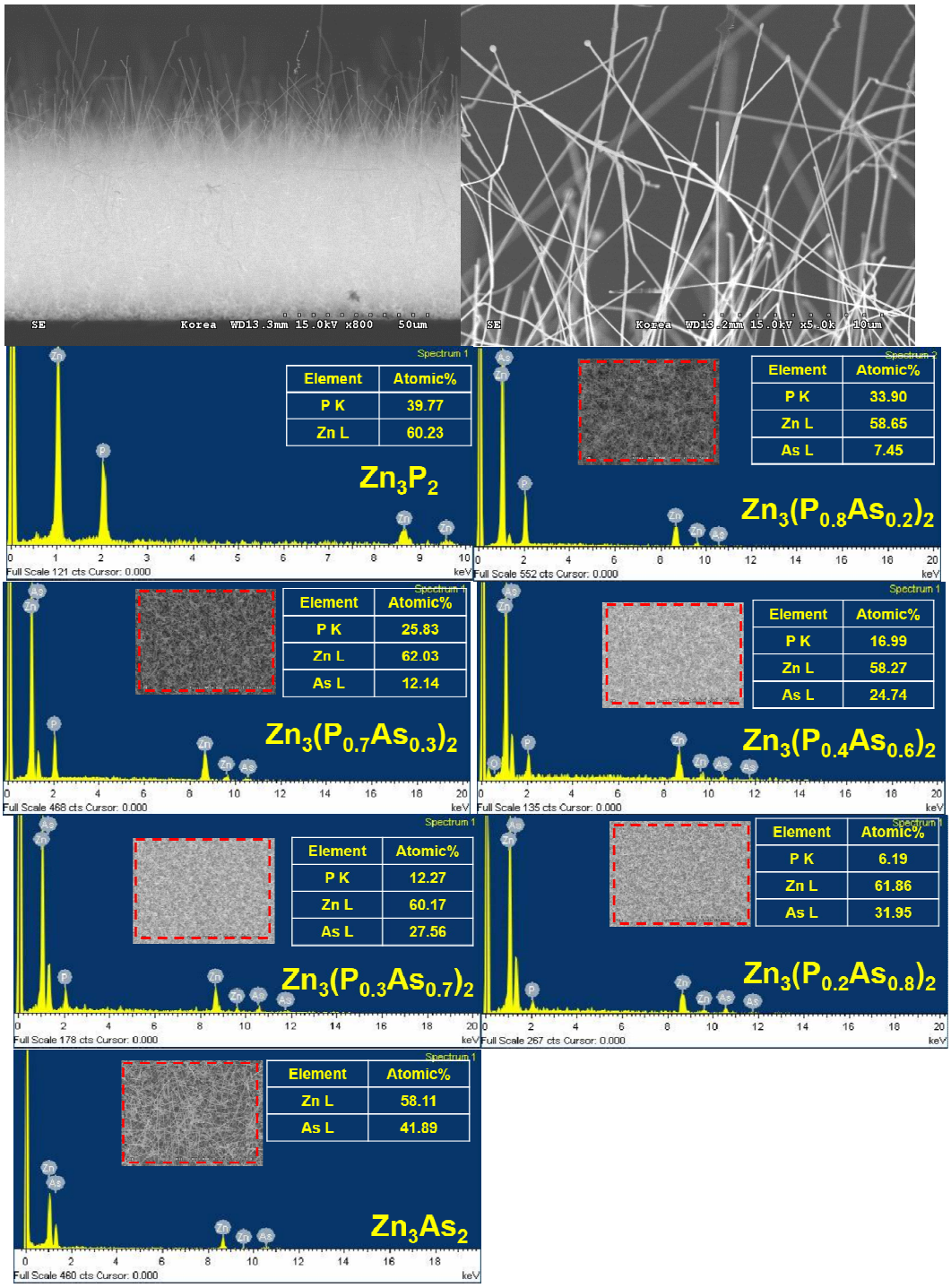

Figure S3. EDX spectra of S-$Zn_3(P_{1-x}As_x)_2$ NWs: x = 0, 0.2, 0.3, 0.6, 0.7, 0.8, and 1. The corresponding HAADF STEM images are shown in the insets. The composition was calculated using the Zn L shell, P K shell, and As K shell peaks.

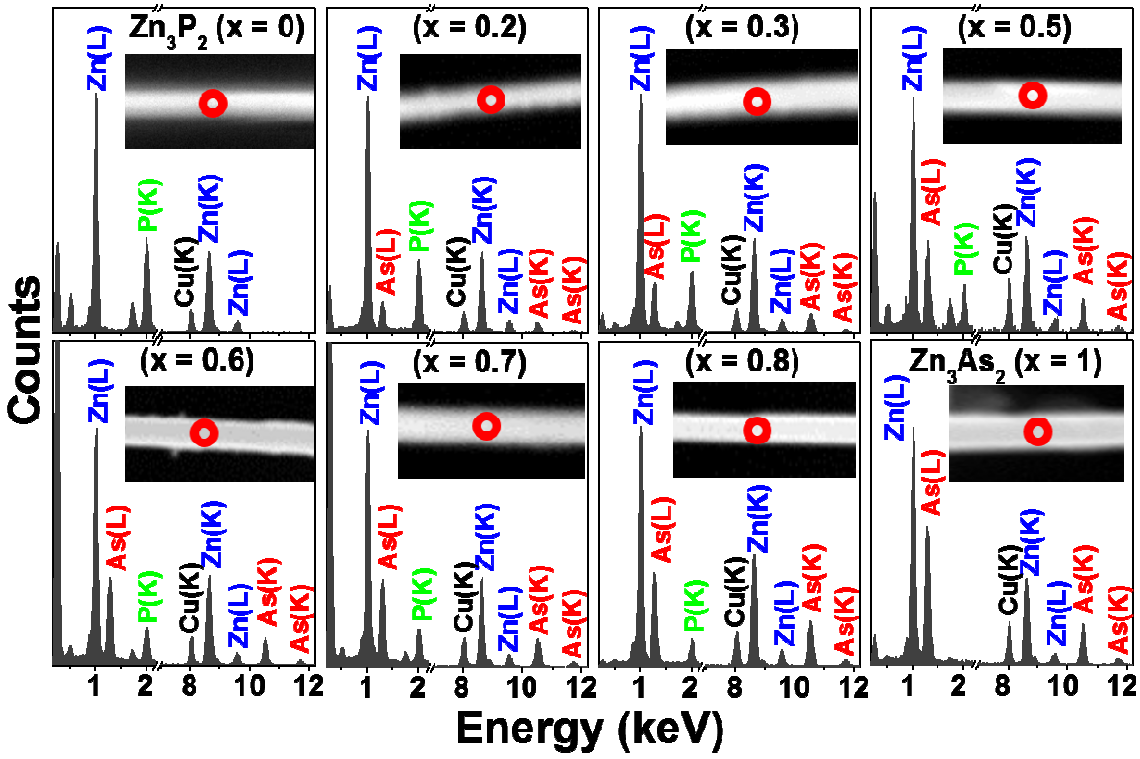

Figure S3. HRTEM images (zone axis = [01$\bar{1}$]) of the catalyst-NW interface for the S-Zn_3P_2 NWs with the [011] growth direction. The Au-NW interfaces consisted of the (111) and (100) planes, where the latter planes are encapsulated by the NWs. This morphology increases the interfacial area and drives the nucleation of the (111) planes to enable the NW growth along the [110] direction.

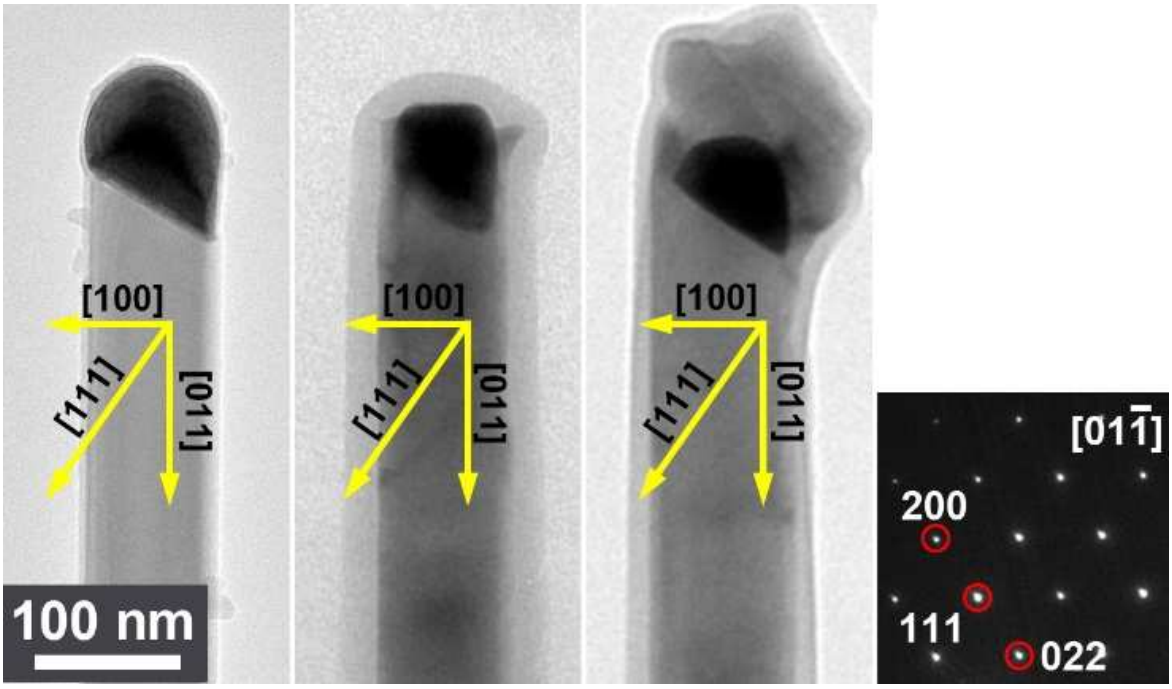

Figure S4. XRD patterns of the T-$Zn_3(P_{1-x}As_x)_2$ NWs, for x = 0, 0.1, 0.5, 0.9, and 1. As x increases, the peak becomes broader initially and then narrower. The superlattice structures likely induce a wider distribution of the lattice constants, which increases the width of the XRD peak.

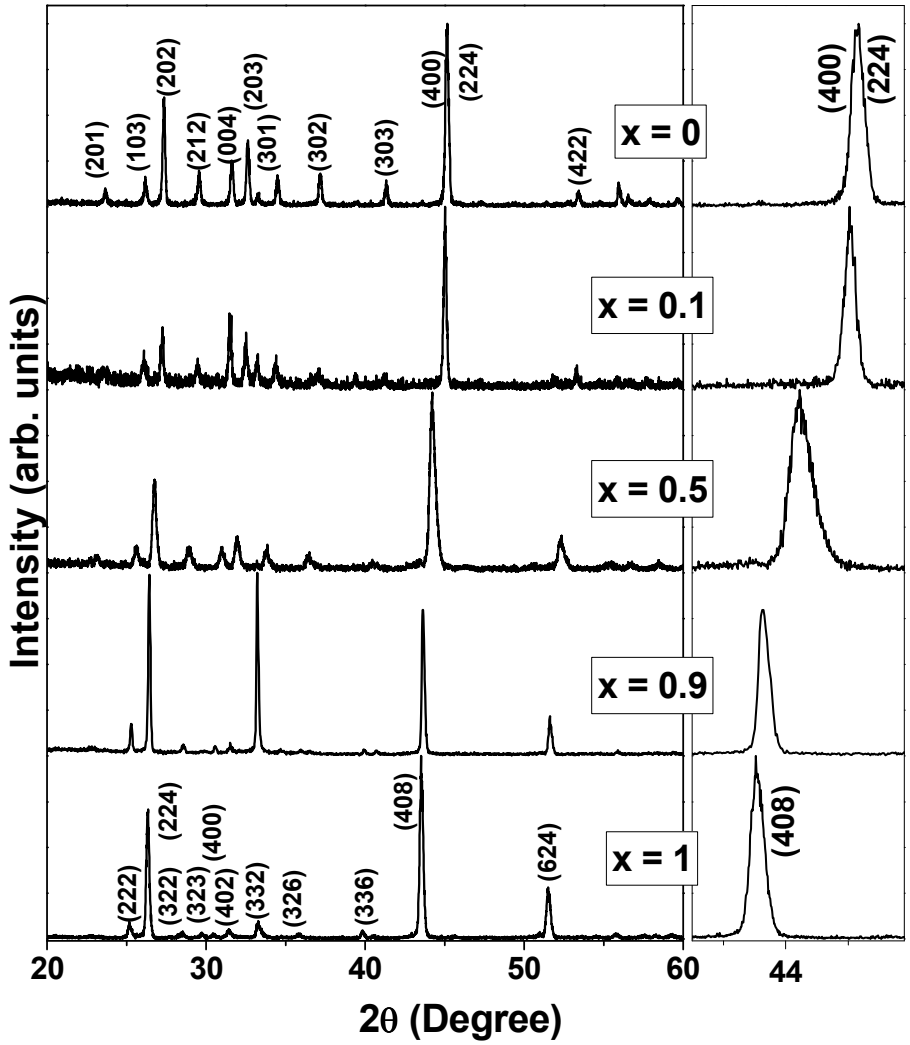

Figure S5. EDX spectra of single T-$Zn_3(P_{1-x}As_x)_2$ NWs whose STEM images are shown in the insets: x = 0.1, 0.5, 0.9, and 1. The composition was calculated using the Zn L shell, P K shell, and As K shell peaks. The Cu peak is orginated from the Cu TEM grid.

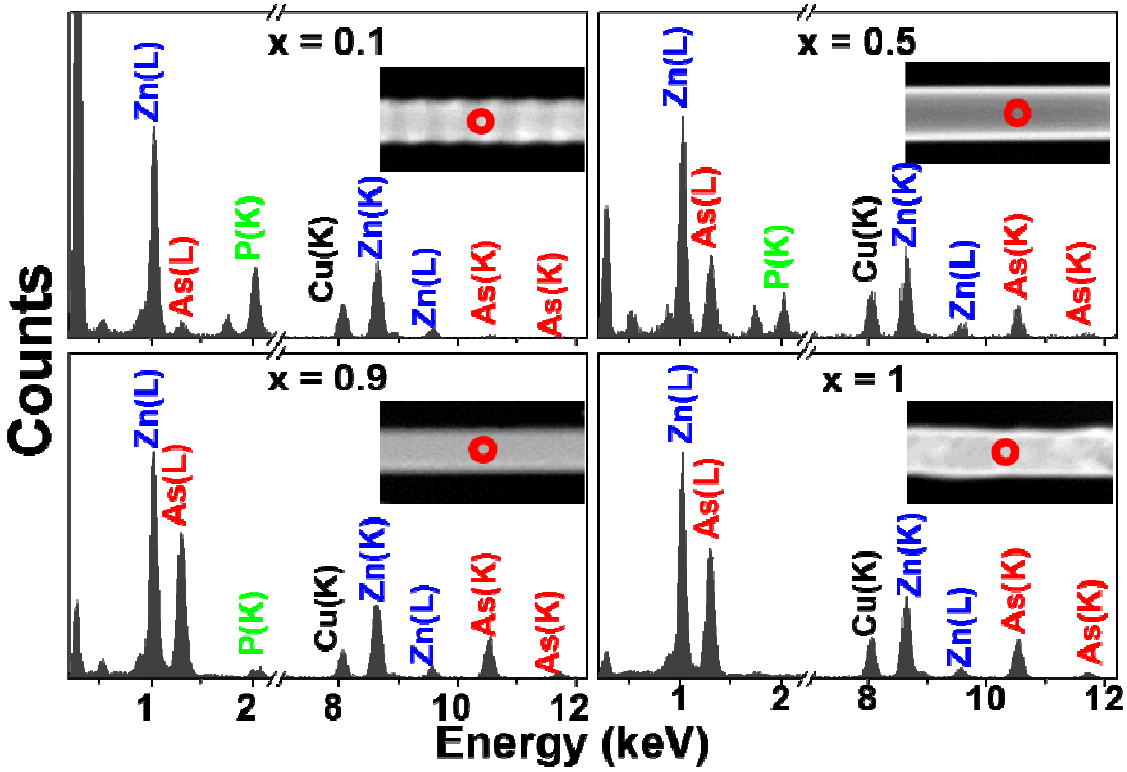

Figure S6. Schematic model of the twinned superlattice structure; the twin octahedral slice blocks have six equivalent ⟨112⟩ apexes, and stack with alternating orientations along the [111] direction. The six side facets of the blocks are enclosed by the {112} surfaces. For the sequential 30° turns, the top and side views are displayed. When the incident electron beam is projected at the ⟨112⟩ zone axis, the apexes become collinear, so the straight morphology appears. At the ⟨011⟩ zone axis (30° turn), the two apexes stick out, resulting in the zigzag morphology.

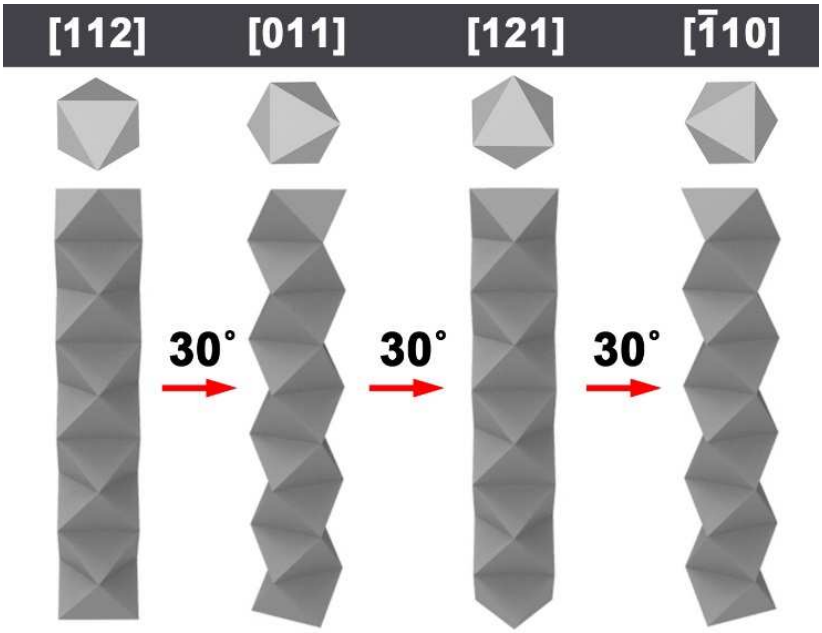

Figure S7. (a) UV-visible diffuse reflectance spectra (absorption) and K-M plots (b) $[F(\nu)h\nu]^{1/2}$ and (c) $[F(\nu)h\nu]^2$ *versus* $h\nu$ for T-$Zn_3(P_{1-x}As_x)_2$ NWs (x = 0, 0.3, 0.6, 0.7, 0.8, and 1). (d) Band gaps of the NWs, as determined by the onset of the UV-visible spectrum and the K-M plot (indirect/direct) *versus* the As content (x). The direct band gap shows a concave optical bowing with a negative bowing constant b (= -0.090 eV). This reduced nonlinear feature (b = 0.185 for S-$Zn_3(P_{1-x}As_x)_2$ NWs) was probably related with the defect sites of the polytypic structure.